AIAA SciTech Forum
23-27 January 2023, National Harbor, MD & Online
AIAA SCITECH 2023 Forum

10.2514/6.2023-0839

Uncertainty Quantification of a Parallel Hybrid-Electric Propulsion EPFD Vehicle

J.Uzodinma*, T. Zaidi†, M. Walter‡, R. Gautier§, and D. Mavris¶
The Daniel Guggenheim School of Aerospace Engineering
Georgia Institute of Technology, Atlanta, 30332, USA

The NASA Electrified Powertrain Flight Demonstration (EPFD) program is a collaboration between industry and academia to accelerate the development and implementation of megawatt-class power systems in commercial aviation. Technology development programs are often associated with cost, performance, and schedule risks, which can result from technical uncertainty. To assess and offer insight to effective mitigation of risks associated with the NASA EPFD program, an uncertainty quantification analysis for future hybrid-electric commercial aircraft is addressed. An uncertainty analysis is presented for the electrified aircraft propulsion systems of a 150-passenger hybrid-electric aircraft model. Uncertainty at the component-level of the powertrain system is considered and its effect is propagated to vehicle-level metrics. The primary focus is identifying and assessing the key uncertain technological inputs driving the variability of the vehicle's performance responses.

I. Introduction

As government agencies and regulatory bodies around the globe focus on emission reduction efforts to address climate change, the aviation industry is in need of change in order to assist these efforts. Currently, the aviation industry contributes around 2% of CO_2 emissions globally [1], and with projections of rapid growth in air travel over the upcoming decades, aviation's CO_2 contributions could grow to more than double of their current level by 2050 [2]. International initiatives have been outlined to combat the harmful environmental effects of this projected growth in air travel. In 2019, the International Civil Aviation Organization (ICAO) set aspirational targets for emission reduction by 2050, and achieving these targets requires improvements in engine technology and aircraft performance as well as changes to aviation operations as a whole [3]. While growth of sustainable aviation fuel usage is expected to play a large role in the aviation industry approaching emissions goals, the infusion of advanced technologies is still indispensable to realizing an environmentally-sustainable aviation industry.

Advanced aircraft technologies, such as hybrid-electric propulsion (HEP), have been proposed as possible solutions to curb harmful emissions from the already vast and fast-growing aviation industry. HEP merges the benefits of internal combustion engines and fully-electric propulsion architectures. HEP can utilize both fuel and batteries for energy storage, which allows for reductions in fuel burn when compared to traditional internal combustion engines used on today's airliners. Other potential benefits are decreased noise pollution, lower maintenance, and improved safety [4]. The development and deployment of a viable single-aisle, hybrid-electric passenger aircraft greatly depends on advances of electrical hardware such as batteries, motors, inverters, generators, etc. Projections of technological advancement have inherent uncertainty, as major breakthroughs as well as extensive hiatuses between key advancements cannot be precisely forecast. Thus, for the development of megawatt-class hybrid-electric aircraft suitable for aviation's stakeholders, including passengers, airlines, and regulatory agencies, uncertainty quantification (UQ) is needed to assess risks and to inform further research & development efforts.

The aim of this paper is to disseminate the findings of the UQ analysis for the NASA EPFD program. The interest is to understand and to quantify how uncertainty in technological parameters affects variability in vehicle performance metrics. Therefore, the current study focuses on sensitivity analysis. Specifically, two studies are carried out. The first

*Graduate Research Associate, School of Aerospace Engineering, Georgia Tech
†Lecturer and Research Engineer II, School of Aerospace Engineering, Georgia Tech
‡Research Engineer II, School of Aerospace Engineering, Georgia Tech
§Postdoctoral Fellow, School of Aerospace Engineering, Georgia Tech
¶S.P. Langley Distinguished Regents Professor and Director, School of Aerospace Engineering, Georgia Tech, AIAA Fellow

one concerns with the lack of knowledge on defining uncertain parameters; therefore, studying the robustness of the sensitivity analysis against distribution type is of importance and is thus addressed. The other study examines how uncertainty in technology forecasts can affect the sensitivity analysis; thus, technology projections for a few vehicle model inputs are implemented in the study.

The current article is organized as follows. In Section II, a description of our technical process for approaching the UQ analysis is presented. Section III provides specifics on the formulation of the methods employed as well as EPFD performance model. Results are shown in Section IV, while conclusions are lastly provided in Section V.

II. Methodology

A. Problem Description

The current study aims to estimate the variability of EPFD vehicle-level performance metrics due to technological parameters modeled as uncertain. The UQ process is illustrated in Figure 1. The inputs of the EPFD model are divided in two groups: deterministic inputs and uncertain inputs. Deterministic variables can either be design variables or operational parameters. These variables are fixed to specific values during the UQ analysis since they are not affected by technological uncertainty. Uncertain variables represent parameters stemming from evolving technologies, which are not precisely known; however, their impact on the EPFD vehicle performance is of interest. Accordingly, these variables are modeled as varying randomly according to a probability density function. Propagating the values of these uncertain inputs through the EPFD vehicle model then results in uncertain performance responses.

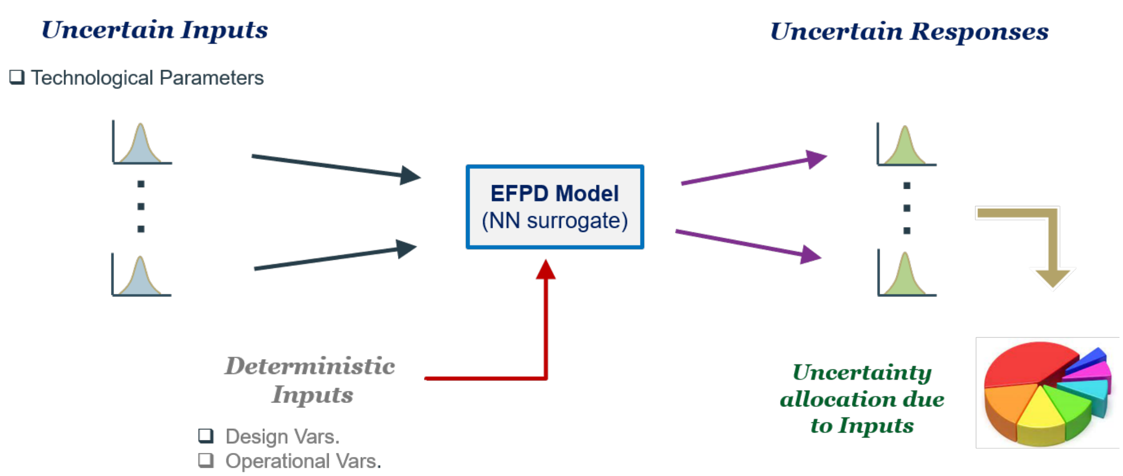

Fig. 1 UQ proccess on EPFD model

The total response uncertainty can be divided according to the contribution from each uncertain input. The study of allocation of response uncertainty to these inputs is the main objective in the present study. Examination of such uncertainty allocation is of relevance since it allows to identify the largest input contributors to response variability. In turn, this may assist the selection of a subset of technologies that have the greatest impact on vehicle-level performance. Accordingly, these technologies may be given particular attention as part of the development effort.

B. UQ Studies

The focus of the present UQ analysis is examining the effect of technical uncertain parameters on the variability of the EPFD vehicle performance. The main purpose is to identify the main contributors to performance variability so that development effort can be placed on those particular technologies. As previously stated, the UQ analysis in the current study consists of two aspects. The first aspect focuses on examining the robustness of the sensitivity analysis against the lack of knowledge on defining uncertain parameters, and the second aspect addresses the effects of uncertainty forecasting of few technologies on the sensitivity analysis. Before addressing these two aspects of the current UQ study, it is convenient to examine the variability of the EPFD performance responses due to all model inputs.

1. Baseline sensitivity study

A preliminary analysis of the vehicle model's variability due to all its inputs is conducted first. The intention is to estimate the respective contributions of the two groups of inputs - deterministic and uncertain. The inputs in the deterministic group such as design and constraint variables can mask or hide the impact of the technical uncertainty variables, which are of primary interest. The goal is to eventually eliminate the masking effect of design and constraint variables. Therefore, as a reference, a sensitivity study on all inputs - deterministic as well as uncertain - is carried out. This reference study assumes minimal knowledge about the system inputs and varies all input values uniformly across the full range of the design of experiments (DoE) used to train the surrogate models. In other words, the minimum and maximum values of each uniform distribution matched the respective input's minimum and maximum values from the DoE. This initial Baseline Sensitivity Analysis study will serve as a reference point for the main UQ studies conducted in this work.

2. Study A: Impact on sensitivity due to distribution type

The results on the sensitivity analysis critically depend on the choice of the probability density function of the uncertain input variables. Nevertheless, complete definition of uncertainty sources - support as well as type of distribution of the random variables - is not always possible, resulting in a lack of knowledge on the uncertain inputs. Therefore, analyzing the impact of the type of probability density function on the sensitivity indices is a relevant question. Consequently, the effect of using different types of input distributions on sensitivities of EPFD responses is examined. All deterministic variables - design and constraint parameters - are fixed at predetermined optimal values based on best fuel consumption configuration, rather than being allowed to vary over ranges. Three distribution types are utilized. These are uniform, triangular, and truncated normal, which can reflect different levels of knowledge about the projected values of each input.

3. Study B: Impact on sensitivity due to technology forecasting

In the previous study, the ranges used for technical uncertainty variables were set by the bounds of the DoE. Employing information from technological projections would allow for more informed ranges for the uncertain variables of interest, which increases the utility of the UQ study. Therefore, technological projections are used to inform ranges for technological metrics regarding battery cells, electric machines, and power converters. Because of variance in technological projections, which arises from the relative aggressiveness or lack thereof present in projections, three scenarios were developed for this Study. For the specific energy of future battery cells, projected values from [5] were implemented into this study. These projections were developed using an S-curve projection to fit historical data of battery cell-level specific energy and to project cell-level specific energy improvement over the coming decades, and Figure 2 shows curves representing conservative, nominal, and aggressively projections.

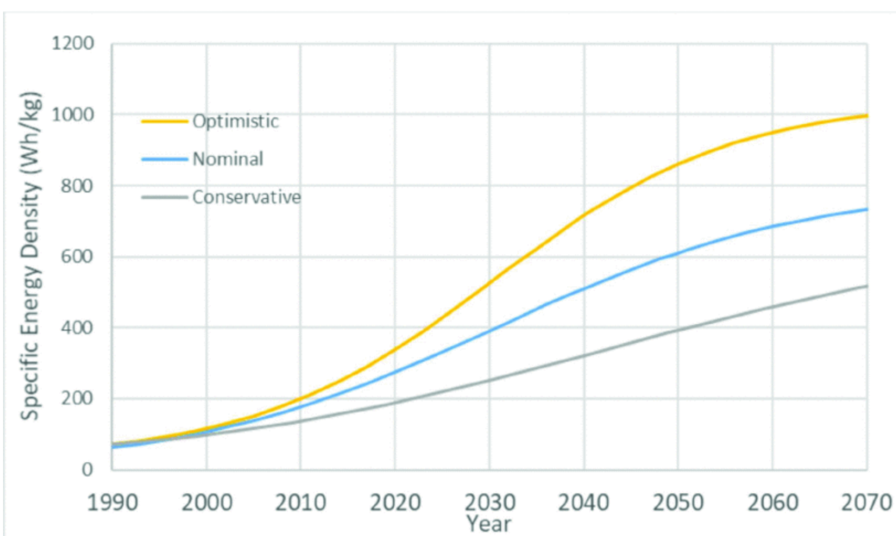

Fig. 2 Battery Specific Energy Projections [5]

In a similar manner, conservative, nominal, and aggressive projections from [6] and [7] were leveraged to define ranges for specific power of future electric machines and power converters. These projections were developed using historical data and logistic fits with inflection points at the years 2020, 2030, and 2040, which respectively correspond to conservative, nominal, and aggressive projections. Figures 3 & 4 show the respective curves generated in this process. Finally, because historical data for efficiencies of future electric machines and power converters was too scattered and haphazard for logistic fitting, projections for efficiency were generated using state-of-the-art (SoA) values as initial points and implementing an annual reduction in losses, and the magnitude of the annual reduction in losses would correspond to relative aggressiveness or lack thereof present in the projections [6, 7].

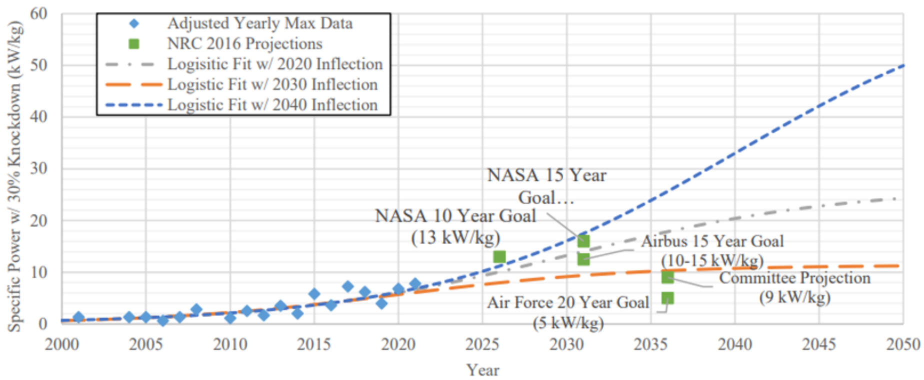

Fig. 3 Electric machine specific power projections using logistic fits [7]

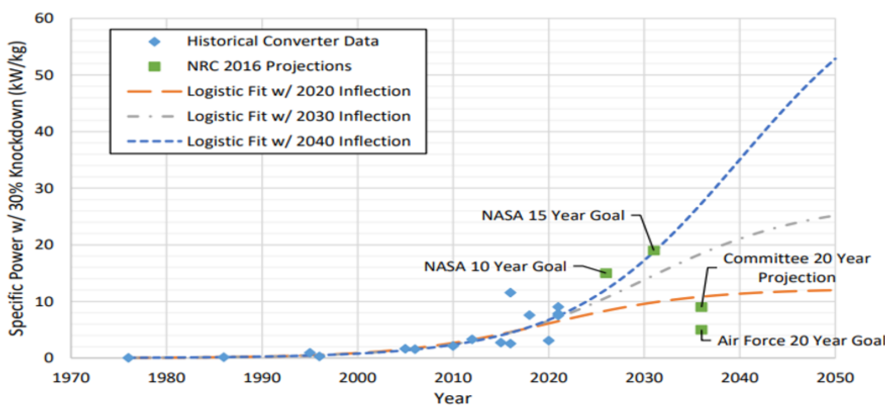

Fig. 4 Power converter specific power projections using logistic fits [6]

The resulting projections for the years 2030, 2040, and 2050 are shown in Table 1. As can be seen, three different projected values were obtained for each year based on conservative, nominal, and aggressive estimates respectively. These values were used as inputs to the simulation to obtain more accurate uncertainty distribution projections. In this case, projected values were input as triangular distributions with available conservative estimates serving as the lower bound, nominal estimates serving as the peak values, and aggressive estimates serving as the upper bound. Design and constraint variables were once again held constant at their optimal values. Since projections for the remaining technical uncertainty variables was not considered at this point, the distributions for these variables remained uniformly distributed across their entire range. This study is further divided into three cases for the years 2030, 2040, and 2050.

Table 1 Projected parameters for battery cells, electric machines, and power converters

Time Frame	Confidence	Battery Cell-Level Specific Energy (Wh/kg)	Electric Machine Specific Power (kW/kg)	Electric Machine Efficiency (%)	Power Converter Specific Power (kW/kg)	Power Converter Efficiency (%)
2030	Conservative	359	9.2	0.963	9.6	0.982
	Nominal	489	13.2	0.968	13.8	0.985
	Aggressive	584	16.1	0.974	17.3	0.988
2040	Conservative	459	10.8	0.967	11.4	0.985
	Nominal	638	20.4	0.975	21.1	0.989
	Aggressive	795	33.0	0.983	35.1	0.994
2050	Conservative	561	11.3	0.970	12.0	0.987
	Nominal	764	24.3	0.980	25.2	0.992
	Aggressive	957	50.0	0.989	52.9	0.997

III. UQ Approach and Implementation

The UQ approach involves three main phases: propagation of component-level uncertainty through the vehicle model, probabilistic evaluation of the benefit of hybrid-electric propulsion, and assessment of the variability of the EPFD model with respect to its inputs. These phases are described in more detail next.

A. EPFD Vehicle Performance Analysis Model

The intent of the parallel hybrid electric powertrain is to supplement power generation for the propulsor in a manner that allows for downsizing of the conventional turbofan core while satisfying aircraft thrust requirements and reducing overall vehicle fuel consumption. The NASA EPFD project has modeled several small passenger category aircraft ranging from 19-passenger turboprops up to 150-passenger turbofan architectures with hybrid electric powertrains [8]. The hybrid electric versions of these smaller class vehicles are envisioned as more promising to show fuel consumption advantages over larger category aircraft given current battery technology levels and mission requirements. The models are used to identify optimal performing architectures with respect to key performance parameters of interest. The 150-passenger hybrid-electric aircraft model was chosen in this UQ work for its maturity and availability, and thus, was determined as the most relevant for the development of our approach.

The modeling of hybrid electric powertrains in conjunction with conventional turbofan architectures presents unique challenges from performance and operational perspectives. From a performance view, the aircraft propulsor must be modeled to be driven by multiple energy sources: the conventional fuel source as well as the battery-driven electric motor. Additionally, since the thrust output of the engine is no longer controlled by a single thrust lever which controls fuel flow, there are several new operational modes to consider in which the electrical system can provide power to the aircraft including eTaxi, takeoff boost, climb boost, etc.

The EPFD vehicle model was developed using the Environmental Design Space (EDS) software [9], which is a modeling and simulation environment for aircraft design, performance, and mission analysis. The EDS environment incorporates several analysis modules including NASA codes like NPSS and WATE++. This environment is used to model the hybrid electric architecture with a battery, power converter, and an electric machine in parallel with the turbofan low pressure (LP) and high pressure (HP) shafts. As shown in the hybrid electric architecture schematic below in Fig 5, the parallel hybrid electric architecture includes a common DC battery power source that supplies energy to a power converter and an electric machine on each of the LP and HP shafts. The electric machine can operate as both a motor or a generator depending on the operational mode of the powertrain.

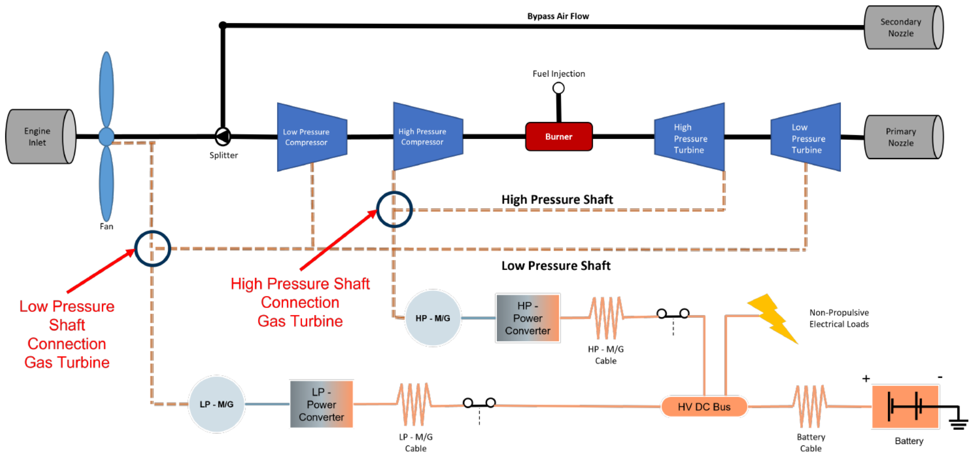

Fig. 5 Parallel Hybrid Electric Architecture Schematic

We draw the reader's attention to the fact that the EPFD project is still underway, and so is the modeling effort. As a result, the specifics of the vehicle model discussed in this section are subject to change in the future. Because the outcome of the UQ studies presented in this paper directly rely on the vehicle model, they are expected to vary when the vehicle model is updated. As such, the UQ results presented in IV, that are based on the version of the EPFD vehicle model available in the Fall of 2022, may be deemed preliminary.

This section provided an overview of the performance model enabling the reader to better understand the UQ analysis that will follow. Interested readers may reference [8] for further details of the performance model and how it was created. While the performance model described above is capable of analyzing different hybrid electric architecture designs, its runtime is too long to enable UQ studies reliant on high sampling of input random variables.

1. Surrogate Model Creation

The EPFD model is not employed directly in the current study. Instead, a surrogate version of it is employed. This is a key enabler for the undergoing work since it allows for fast evaluation, which is essential in UQ studies where sampling approaches are employed, thus needing very large number of model evaluations. Artificial neural networks (ANN) models were trained using data generated using the EPFD model. The architecture of ANN surrogate models is made up of two inner layers and the hyperbolic tangent function is used for the nodes' activation functions. A distinct surrogate model for each of the six responses of interest, as opposed to using a multi-output ANN. These responses are listed in Table 2 below:

Table 2 Responses

Name	Unit	Description
Design OEW	lbs	Design Operating Empty Weight
Design TOGW	lbs	Design Takeoff Gross Weight
Δ Block Fuel 900	%	Percentage Change in Block Fuel for a 900 nmi Mission for Hybrid Vehicle Relative to Baseline
KPP-1	kW	Key Performance Parameter for the Total Power Level of the Integrated MW-Class Powertrain System
KPP-2	kW	Key Performance Parameter for the Individual Power of Electric Machine
KPP-5	kW/kg	Key Performance Parameter for the Specific Power of Electric Powertrain

The vehicle model has a total of 34 inputs. A detailed description of all these inputs along with their corresponding ranges is shown below. As discussed previously, inputs are grouped depending on whether they are treated as deterministic or uncertain. The grouping process begins by separating the inputs according to their function on the performance model as follows:

- *Deterministic Design and Operational Variables* : their values are usually decided upon early in the design process or are restricted based on physical, technological, or functional requirements;

- *Uncertain Technological Variables*: their values are affected by technology readiness and thus remain uncertain for most of the development process and can greatly affect the output variability.

An example of a design variable is the power shave fraction for the hybrid-electric propulsion. Its value is determined from design requirements and trade studies, whereas an example of a constraint variable is battery cable length, which is related to the physical constraints of the aircraft and not technological development. It is noted that these two types of variables are treated as deterministic in studies A and B. When fixed, these deterministic variables are held to their optimum values shown in Table 3. On the contrary, specific energy of future batteries is an example of a technical uncertainty variable, as the state of the art for battery technology in future decades is directly related to technological development. It is therefore treated as uncertain in studies A and B.

Table 3 Surrogate Input Descriptions and Ranges

Variable Name	Description	Min	Max	Optimum
Deterministic Inputs:				
TWR	Thrust loading	0.25	0.37	0.307
WSR	Wing loading	105	158	120.621
PowerShaveFrac	Reduction of core size relative to baseline	0.05	0.8	0.05038
DesPowerRatio	Split between HP and LP motor powers	0.1	1	0.10027
T4margin	Difference in T4 between max takeoff thrust (MTO) and max continuous thrust (MCT)	-400	-150	-263.7099
FPR	Fan pressure ratio	1.35	1.6	1.35015
Ext Ratio	Extraction ratio	0.9	1.4	1.2380856
T4max	Turbine inlet temperature	3000	3600	3541.9346
HPCPR	Pressure ratio of the high pressure compressor	12	19	15.705897
OPRD TOC	Overall pressure ratio at top-of-climb	45	65	48.709362
HPC_Deff	High pressure compressor efficiency delta at aero design point	0.0028	0.033	0.0028
HPC_s_Wt	High pressure compressor weight scalar	0.8	1	0.9
BattFinalSOC	Battery final state-of-charge	0.1	0.2	0.2
ClimbRateFloor	Floor climb rate for determining when boost is necessary	500 3000	1706.2007	
Matched Altitude	Altitude below which vehicle must match baseline climb rate	2000	10000	10000
eTaxi Duct15 PressureLoss	Bypass duct pressure loss during the eTaxi calculations	0	0.01	0.0025
ElecVoltage	Battery stack design voltage	500	1500	1008.3003
Batt Cable Length	Length of battery cables	25	75	60
Cable Wire Diameter	Diameter of the individual strands of wire in the cable	20	50	35.916
RAT Weight	Weight of ram air turbine system	92.3	277	184.635
IDG Weight	Weight of integrated drive generator system	113	337	224.85
ATS Weight	Weight of air traffic service system	34.4	103	68.828
Uncertain Inputs:				
Battery Specific Energy	Energy capacity per unit weight of the battery	250	1000	
Elec. Machine Specific Power	Specific Power at Electrical Design Point	3	30	
Power Converter Efficiency	Power loss over the power converter	0.95	1	
Bus Efficiency	Efficiency of the bus	0.95	1	
Electric Machine Efficiency	Efficiency at Electrical Design Point	0.95	1	
Power Converter Specific Power	Used in weight calculation of the power converter based on max power of the electric machine	5	50	
Elec. Machine Cable Efficiency	Defines maximum voltage drop across each cable	0.95	1	
Battery Cable Efficiency	Efficiency of the battery cable	0.95	1	
Battery k6	Battery Technology factor on the battery cell capacity	1	2	
Battery k7	Battery Technology factor on the battery cell zero load voltage	1	2	
Battery k8	Battery Technology factor on the battery max continuous current	1	3	
Pack Factor	Factor accounting for packaging material weight of the battery	0.4	1	

2. Surrogate Model Verification

The surrogate inputs represent component and lower-level parameters and variables within the aircraft. Surrogate model fits were assessed by calculating the coefficient of determination (R^2) values and by inspection of actual vs predicted plots, residual vs predicted plots, model fit error distributions, and model representation error distributions. The surrogate models created shown acceptable accuracy with R^2 values greater than or equal to 0.9 and with actual vs. predicted plots showing no signs of underfitting or overfitting. Furthermore, the residual vs predicted plots displayed the error in a random pattern centered around zero, indicating no apparent prediction bias. Finally, the model fit error and model representation error distributions had normal distributions with means approximately equal to zero and standard deviations smaller or equal to one, which are both ideal. A table of the inputs and their respective ranges from the design of experiments (DoE) used for surrogate model training is included in Table 3.

While the accuracy of the surrogates employed to carry out UQ was deemed sufficient in this preliminary study, it is important to recall that it has direct impact on all the results presented here: using a surrogate model effectively introduces some level uncertainty in the predictions. This added uncertainty is a cost paid for enabling large-scale UQ studies that would otherwise be highly impractical to carry out by directly evaluating the computationally costly vehicle model. Because of their importance, approaches to improve the accuracy of these surrogates in the context of the EPFD program are being investigated. One of the main barriers to creating accurate surrogate models is the number of input dimensions: put simply, as the number of input variables increases, a training set of the same size effectively covers a lesser portion of the total input space. Currently, a single set of surrogates is trained and used throughout all studies, whose inputs are the same as the EPFD vehicle model, whether they are deterministic or uncertain. Since deterministic inputs are fixed in studies A and B, surrogate models could alternatively be created that have a lower input dimension, and are therefore expected to be more accurate, assuming a training set of comparable size. These improvements, along with a better quantification of the impact of surrogate uncertainty on probabilistic projections, are the subject of current research. In addition to the fact that the vehicle model is still being refined, this is another reason why the results presented in section IV may be considered preliminary.

B. Evaluation Criterion

In order to examine the benefit of the hybrid-propulsion power plant, several quantities can be examined. The mean and standard deviation of the responses respectively express the average expected values and its spread. The probability of improvement $P[I]$ expresses the portion of the distribution on the improvement side, in other words the benefit measured compared to a baseline value. Note that this value expresses the probability of improving over a baseline value; however, it does not convey an indication as to the expected value of this improvement. To this end, we use the expectation of improvement denoted $E[I]$. This metric provide a measure of the expected benefit (average improvement) over a baseline value as it is defined over the benefit segment. These last two metrics are illustrated in Fig. 6. Several criteria might be defined; however, in this study, the criterion for evaluating benefit is as follow:

$$\begin{array}{rl} \text{Given} & P[I] > \alpha, \\ \text{would like low value} & E[I] < \text{Baseline} \end{array}$$

The above expression ensures that the success of improving - the greater the value of α, the greater level of improving. The second condition implies that the benefit (in average) is as large as possible.

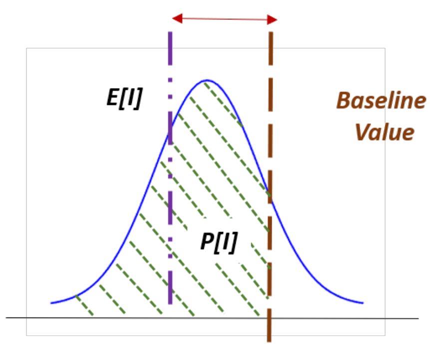

Fig. 6 Metrics for evaluation criterion

C. Variance-based Sensitivity Analysis

A variance decomposition method is employed in the current study in order to assess the variability of the EPFD model with respect to its inputs. The uncertainty on the model outputs results from propagating uncertainties through the model from inputs. Consequently, each input or group of inputs is responsible for a portion of the total response variance. Such a portion when expressed as a fraction can then be used as a metric for measuring sensitivity. This method utilizes repeated function evaluations of the EPFD model, which is aided by surrogate models.

Consider a multivariate function, $f(\boldsymbol{\xi}) = f(\xi_1, \ldots, \xi_d)$, with d mutually independent inputs modeled by random variables, ξ_i, each described by a marginal probability density function $\rho_i(\xi_i)$. Note that the function is strictly deterministic for an instance of the input $\boldsymbol{\xi}^* \mapsto f(\boldsymbol{\xi}^*)$ and thus the function does not possess any aleatoric component. The aforementioned function can then be decomposed [10] by terms of increasing dimensionality as follow:

$$f(\xi_1, \ldots, \xi_d) \;=\; f_0 \;+\; \sum_{1 \leq i \leq d} f_i(\xi_i) \;+\; \sum_{1 \leq i < j \leq d} f_{ij}(\xi_i, \xi_j) \;+ \ldots\; f_{12\ldots d}(\xi_1, \ldots, \xi_d). \tag{1}$$

The component functions on the right side of Eq. 1 are formulated for mutual orthogonality and have null expectation. Expressions for their calculation are given according to the following:

$$\begin{aligned} f_0 &= E[f] \\ f_i(\xi_i) &= E_{\boldsymbol{\xi} \backslash \xi_i}[f|\xi_i] - f_0 \\ f_{ij}(\xi_i, \xi_j) &= E_{\boldsymbol{\xi} \backslash \xi_i, \xi_j}[f|\xi_i, \xi_j] - f_i - f_j - f_0 \\ &\vdots \end{aligned}$$

Expectations, $E_{\boldsymbol{\xi} \backslash \xi_i}$, are defined over all uncertain inputs $\boldsymbol{\xi}$ except ξ_i. Due to orthogonality amongst components in the above decomposition, the total variance of the multivariate function is then simply given by the summation of the variance of each component function - partial variance - as follow:

$$Var(f) \;=\; \sum_{1 \leq i \leq d} Var(f_i) \;+\; \sum_{1 \leq i < j \leq d} Var(f_{ij}) \;+ \ldots +\; Var(f_{12\ldots d}) \tag{2}$$

In the above expression, the first terms $Var(f_i)$ expresses the partial variance due to ξ_i, solely acting on f - portion of the total variance. The second group of terms $Var(f_{ij})$ expressed the portion of the total variance explained by bi-variate contributions from ξ_i & ξ_j, and so on for higher-order terms.

By employing the partial variances, Sobol' indices [10] provide a measure of the sensitivity of the multivariate function f to any combination of the individual inputs. For the univariate contribution, ξ_i, the indices are as follow:

$$S_i = \frac{Var(f_i)}{Var(f)} \tag{3}$$

The above expression is known as the first-order Sobol' index and expresses the ratio of the variance purely due to ξ_i to the total variance, thus $S_i \in [0, 1]$. Note that large values of S_i indicate the importance of ξ_i on the variability of the multivariate function, $f(\boldsymbol{\xi})$. Examining these values is then the focus of a global sensitivity analysis. Moreover, it follows from Eq. 2 that the sum over all Sobol indices results in unity:

$$\sum_{1 \leq i \leq d} S_i \;+\; \sum_{1 \leq i < j \leq d} S_{ij} \;+ \ldots +\; S_{12\ldots d} \;=\; 1 \tag{4}$$

The above sensitivity indices are given by conditional expectations and thus are computationally intensive to calculate. In the current study, the estimators developed in [11] are employed for their calculations.

IV. Results

Results for the UQ studies previously described are presented here. The variance-based sensitivity approach described in the previous section was employed and all the sensitivity indices, S_i, were calculated via the Monte-Carlo (MC) approach with large sample sizes.

A. Baseline Sensitivity Analysis

The Baseline Sensitivity Analysis (BSA) was performed to quantify the uncertainty of the entire input variable space with all input variables characterized uniformly and independently. This provides a useful reference case for comparison and clearer understanding of which input variables are most responsible for the variability of the output responses. The BSA places uniform distributions on all input variables, including deterministic design variables and uncertain technological variables. The range of values for each input distribution corresponds to the ranges used in the DoE used to generate the surrogate's training data. By using uniform distributions on all the input variables, the BSA represents a "maximum uncertainty" case, in which little information is known about the inputs so all input distribution values throughout the range are equally likely. These input distributions are sampled and propagated in Monte-Carlo simulations to generate probability density function (PDF) distributions on the output responses displayed in Figures 7, 8, & 9 .

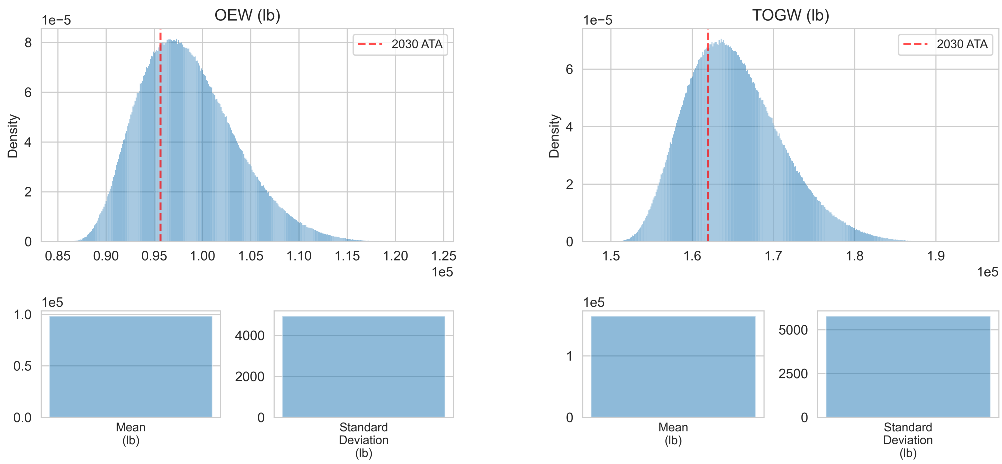

(a) PDF: OEW (b) PDF: TOGW

Fig. 7 PDF response for Baseline Sensitivity Analysis: OEW and TOGW

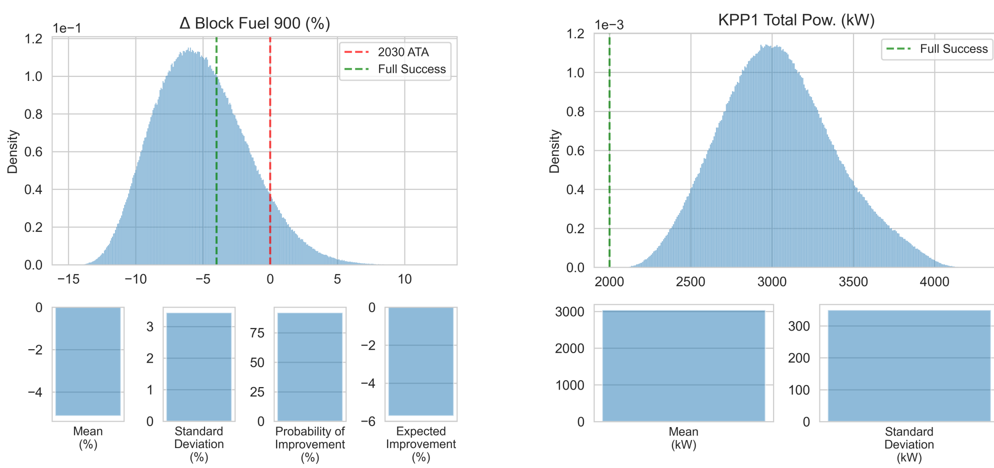

(a) PDF: Δ Block Fuel 900 (b) PDF: KPP1 Total Power

Fig. 8 PDF response for Baseline Sensitivity Analysis: Δ Block Fuel 900 nm mission and KPP1 Total Power

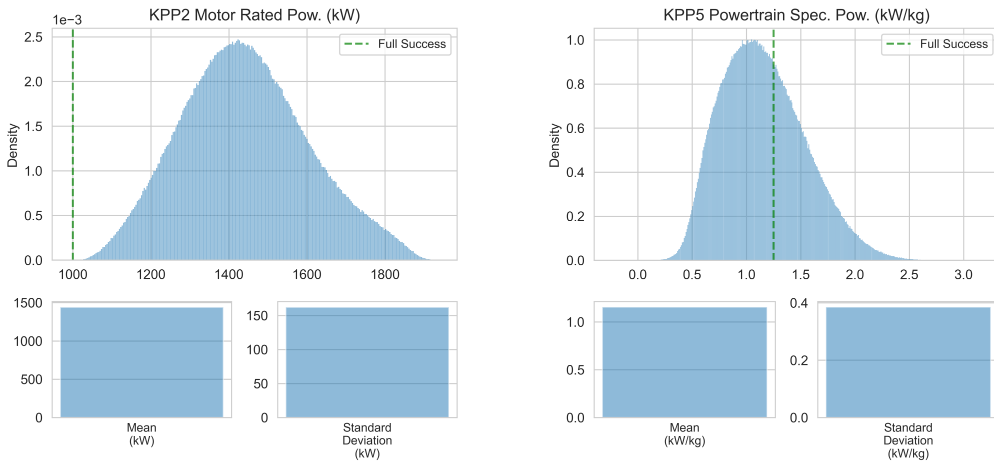

(a) PDF: KPP2 Motor Rated Pow.

(b) PDF: KPP5 Specific Power

Fig. 9 PDF response for Baseline Sensitivity Analysis: KPP2 Motor Rated Power and KPP5 Specific Power

While it is possible to examine the sensitivity of a given response to each individual input variable, it can be more informative to categorize the sensitivities into groupings of 1) deterministic variables, 2) uncertain technological variables, and 3) interactions/higher-order effects. These groupings can help understand which category is driving the variability of each response metrics. Fig. 10 indicates that the deterministic variables are most responsible for the variability of the responses, which is expected. In order to better understand the variability in the responses caused by the uncertain technological variables, Study A and Study B will hold fixed the deterministic inputs at their optimum values while sampling only the uncertain technological variables. These results will be presented in the next sections.

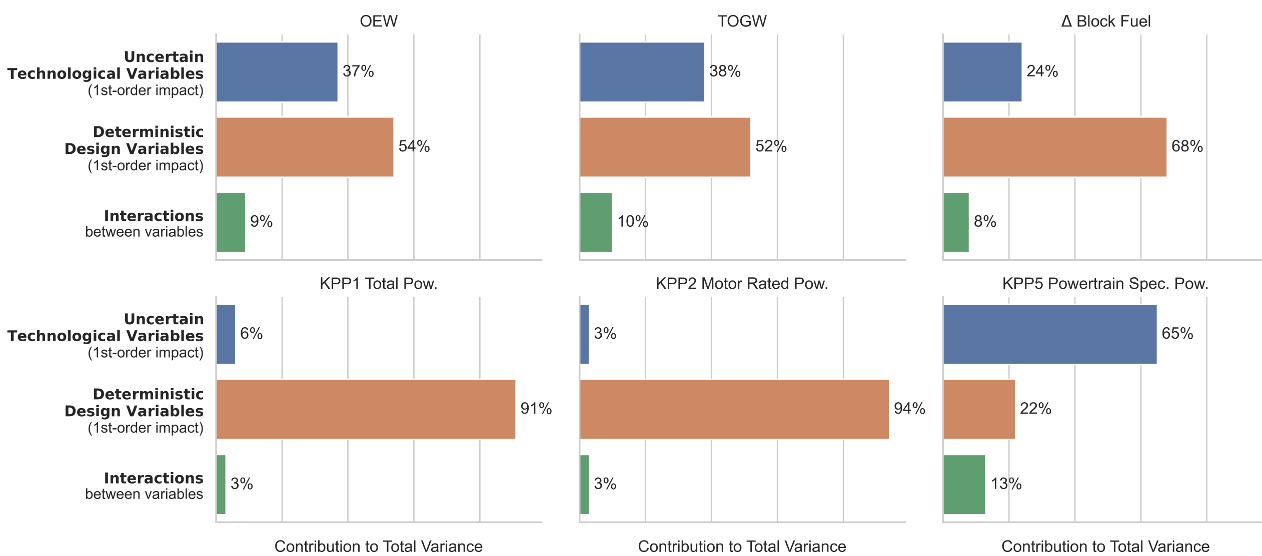

(a) Sobol Index Comparison of Deterministic and Uncertain Variables for Baseline Sensitivity Analysis

Fig. 10 Assessment of Input Contributions in Baseline Sensitivity Analysis

B. Study A: Impact on sensitivity due to distribution type

Probability density functions of all responses with different types of input probability density functions - uniform, triangular and truncated normal - are shown in Figures 11, 12, & 13. In the case of the OEW, TOGW, Δ Block Fuel 900 and KPP2 (Motor Rated Power), the resulting distributions exhibit a noticeable degree of asymmetry with positive skewness, having long tails towards upper values. Conversely, the KPP1 (Total Power) and KPP5 (Specific Power) resulting response distributions are fairly symmetrical for any type of the considered input distribution shape. It is also observed that changing the type of distribution from uniform to triangular and finally to truncated normal results in distributions that are thinner, implying more informative behavior. This behavior is quantified by the value of the variance in bar plot shown below every output distribution.

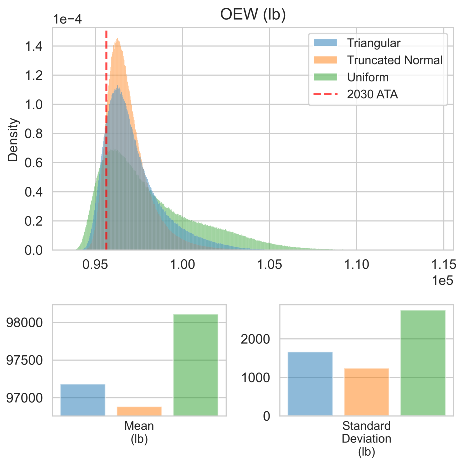

(a) PDF: OEW

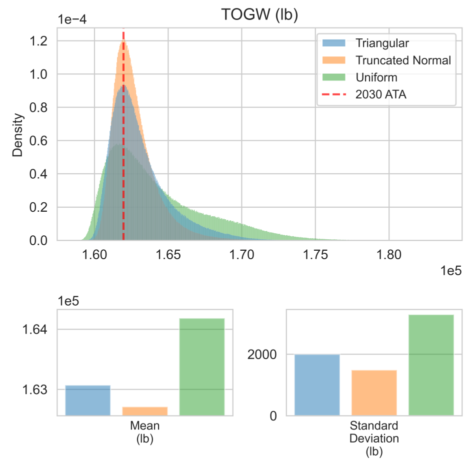

(b) PDF: TOGW

Fig. 11 PDF response for study A: OEW and TOGW

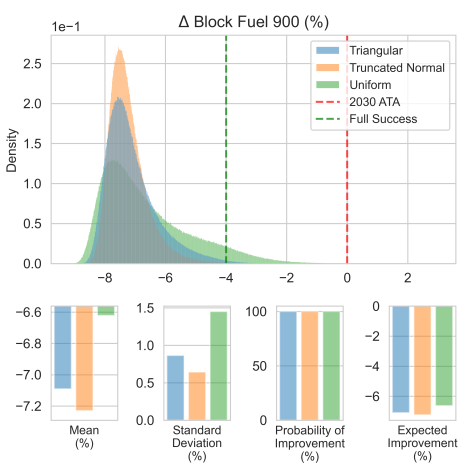

(a) PDF: Δ Block Fuel 900

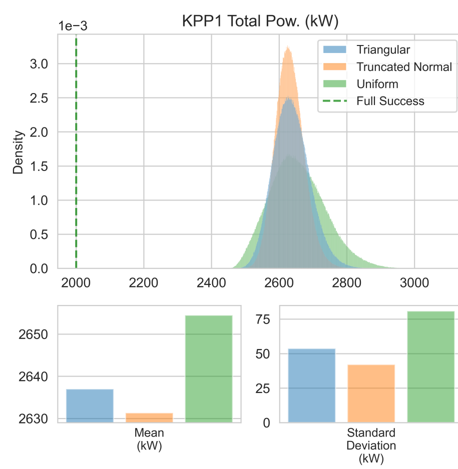

(b) PDF: KPP1 Total Power

Fig. 12 PDF response for study A: Δ Block Fuel 900 nm mission and KPP1 Total Power

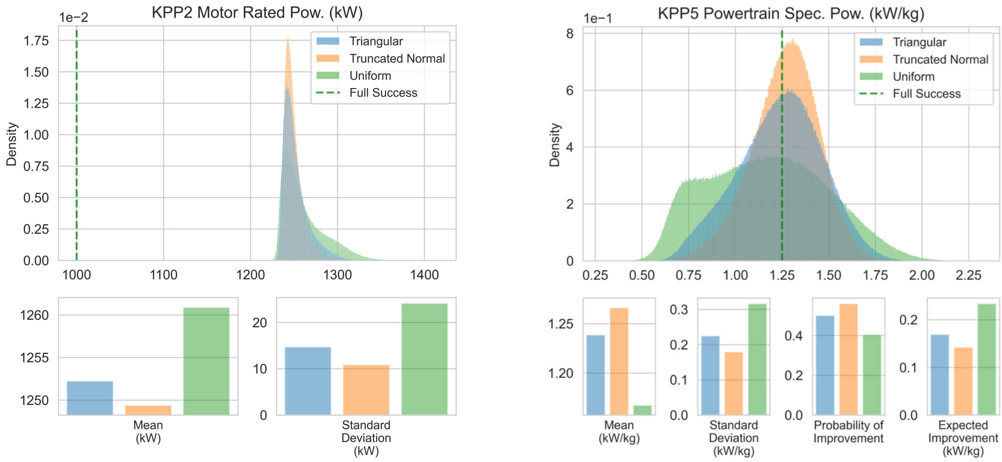

(a) PDF: KPP2 Motor Rated Pow.

(b) PDF: KPP5 Specific Power

Fig. 13 PDF response for study A: KPP2 Motor Rated Power and KPP5 Specific Power

Sensitivity results for all responses in study A are shown in Fig. 14. The value of the first-order sensitivity index S_i (in percentage) - input contribution to the total response variance - is given by the bars. Influential inputs are identified with values of sensitivity index, S_i, above of 4 %. Common influential inputs are consistently battery specific energy, battery k8, electric machine efficiency , electric machine specific power and power converter efficiency. Nevertheless, battery specific energy stands out as the most influential parameters regardless of the input distribution type, with contribution of at least 20% of contribution to the total variance of the responses. The sensitivity study exhibits robustness against changes in the type of probability density function, describing the uncertain inputs. This can be inferred from the results shown in Fig. 14. This figure shows that while the exact amount of variability for each input changes with distribution type, the overall set of inputs driving most of the variability are the same regardless of the employed distribution - uniform, triangular or normal.

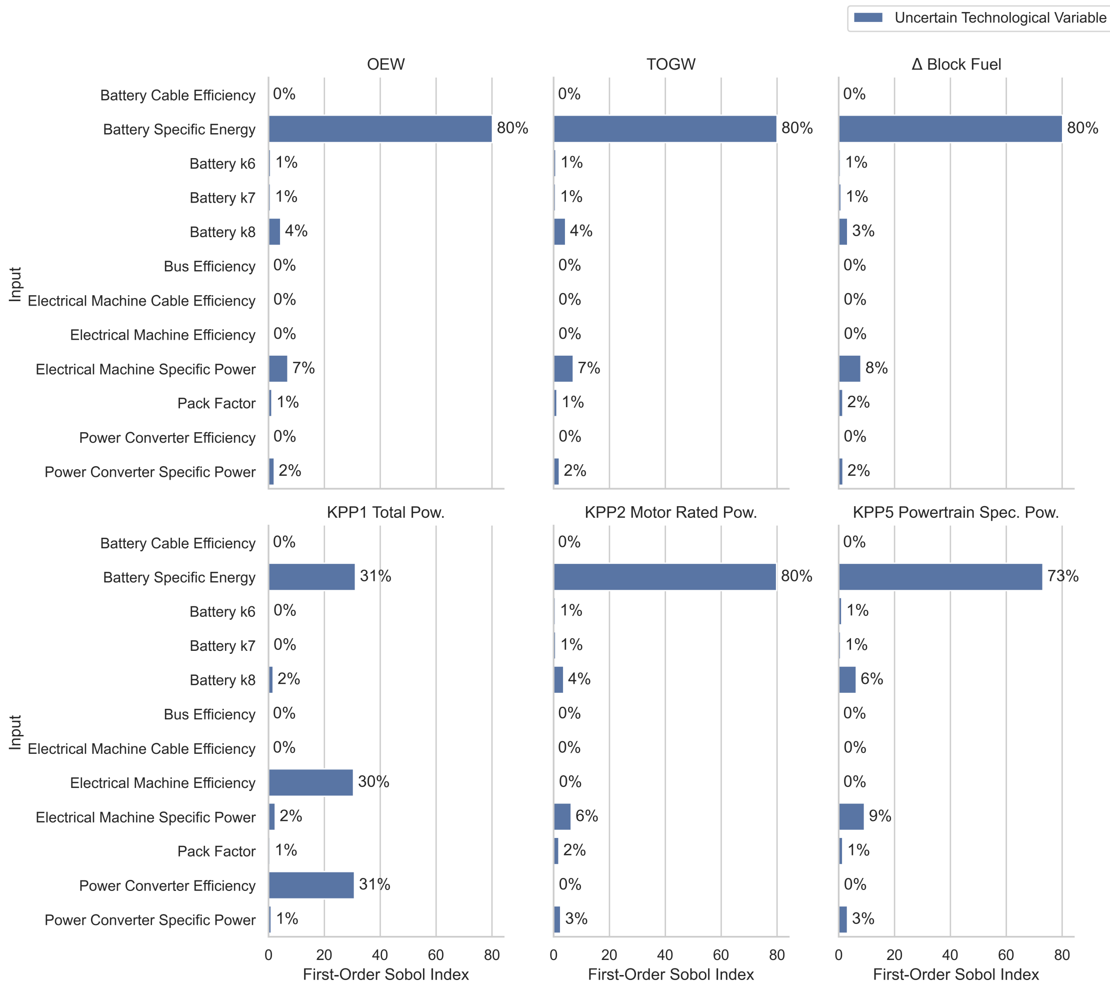

(a) Sobol Indices for Study A: Uniform

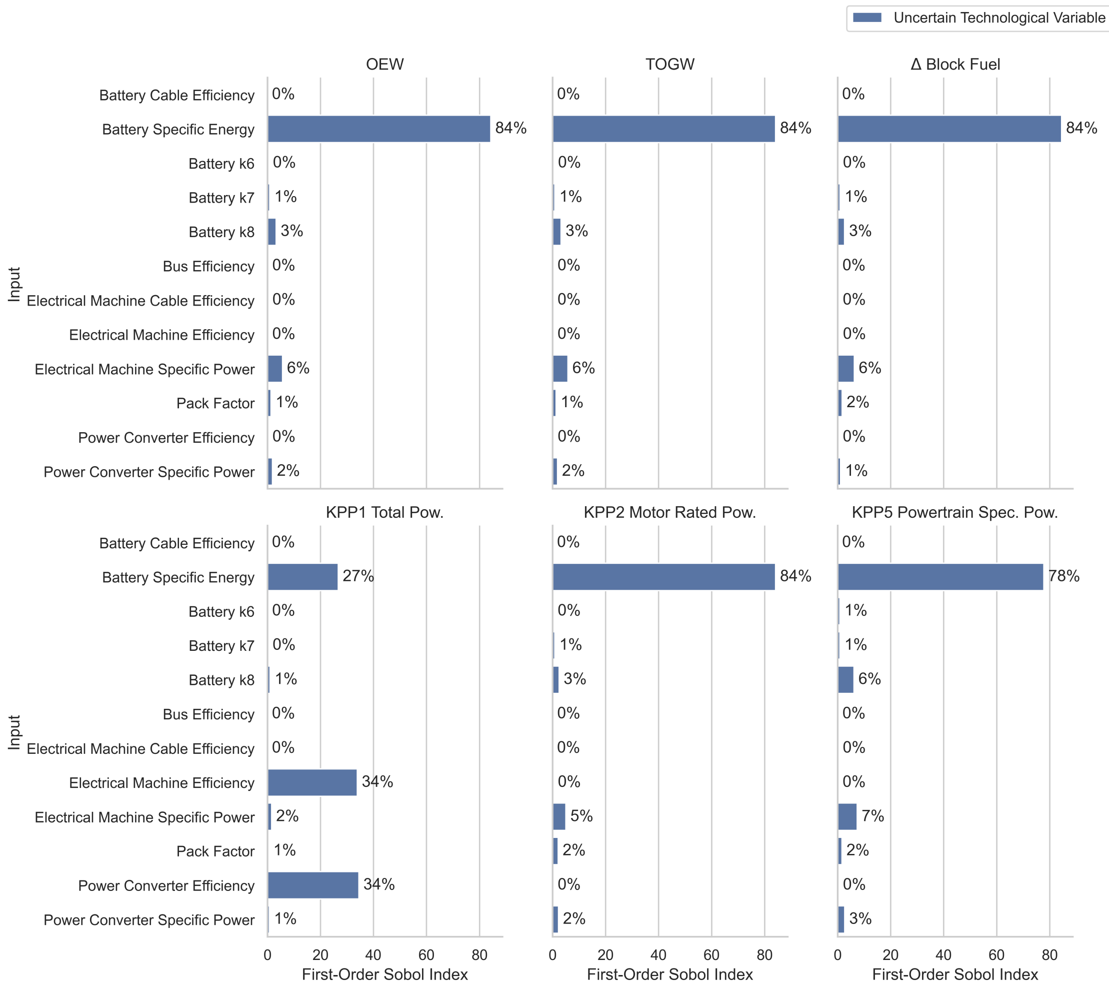

(b) Sobol Indices for Study A: Triangular

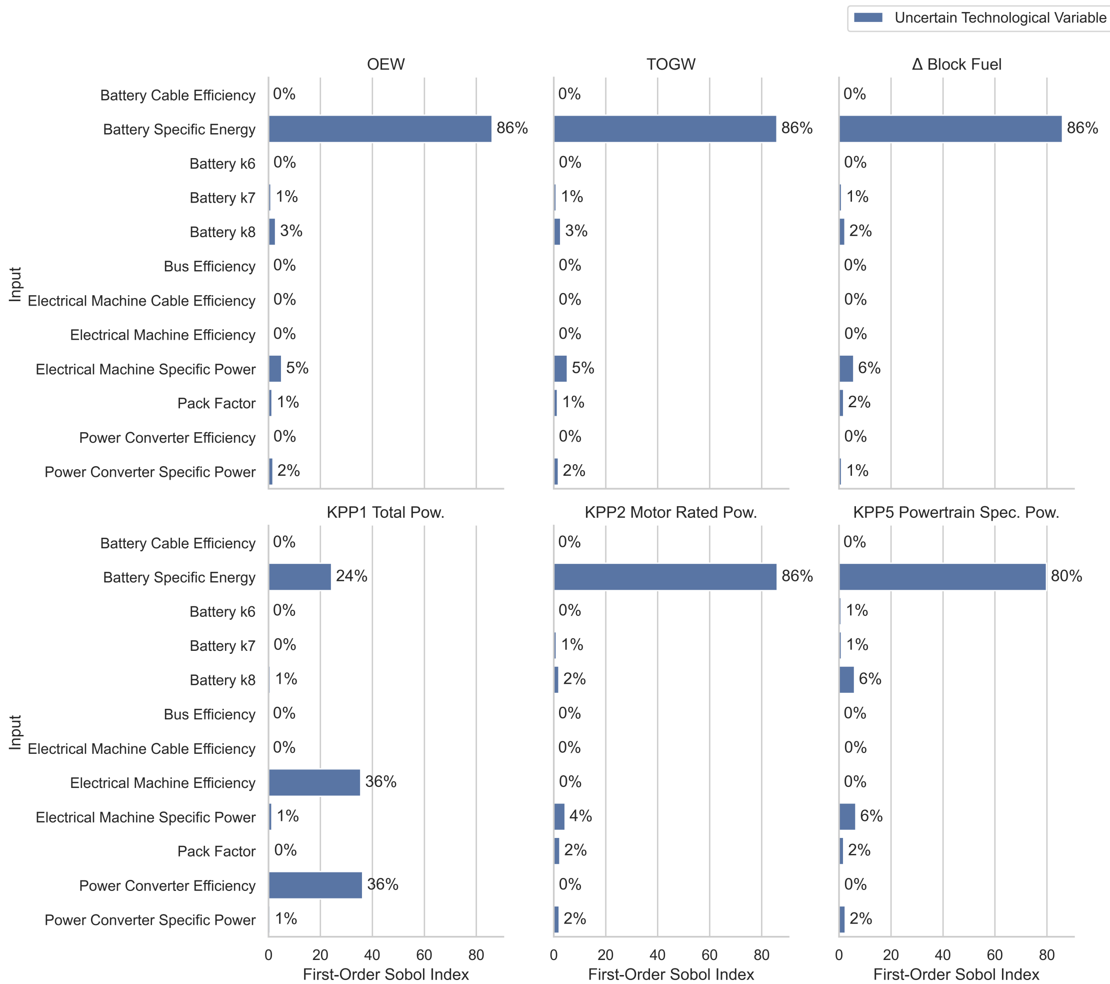

(c) Sobol Indices for Study A: Truncated Normal

Fig. 14 Sensitivity on EPFD responses with different distribution inputs

Moreover, when examining the response distributions for Study A and the results in Fig. 14, it is evident that characterizing inputs with triangular and truncated normal distributions produces similar results. With literature from [12, 13] supporting that triangular distributions are more easily interpreted by subject matter experts, it can be concluded that triangular distributions are a suitable choice for characterization of technological inputs in our UQ study.

C. Study B: Impact on sensitivity due to technology forecasting

With all deterministic design variables held at their respective optimized values, technological projections from Table 1 are integrated into the UQ study. It is important to clarify that technological projections were only utilized for the five inputs included on Table 1, while remaining uncertain inputs are characterized with uniform distributions over their respective DoE ranges. From an assessment of Figures 15, 16 & 17, it can be observed that the standard deviation decreases with time (year) for all responses except KPP5 (Specific Power). This reduction in response standard deviation is related to the nonlinear relationship between battery specific energy and these respective responses. On the other hand, battery specific energy and KPP5 have a relationship that is mostly linear, which is why the standard deviation for KPP5 follows the trend of the input variables' standard deviations. Additionally, in reference to the baseline and success metrics shown on the plots in Figures 16 & 17, more technological development in electrical components allows for a higher probability of improvement or success, which is expected. A more noteworthy observation is technological progress that aligns with the projections in Table 1 specifically yields a 150-passenger class hybrid-electric aircraft that not only reduces fuel usage relative to a traditional ICE aircraft in 2030 but rather, even when considering technological uncertainty, meets the fuel usage reduction target set by NASA.

Moreover, the expected value of this fuel usage reduction or any other response can be determined from an analysis of the successful region of the response's PDF. The Δ Block Fuel 900 response shows output distributions in each time frame that indicate the expected improvement over the 2030 Advanced Technology Aircraft (ATA), instead of today's current technology. Therefore the expected improvement is not indicating the reduction in fuel consumption between a given time frame's EAP vehicle and current aircraft, but rather the difference between a 2030 ATA powertrain and its hybrid EAP vehicle counterpart.

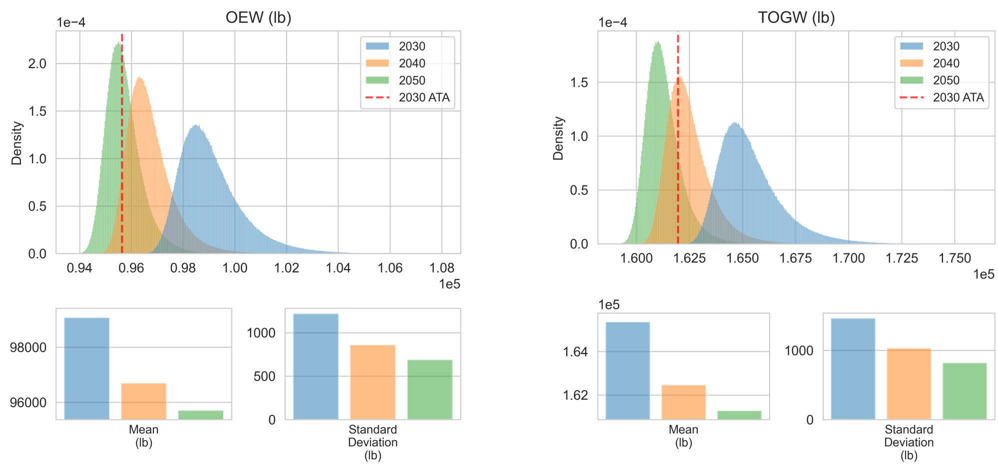

(a) PDF: OEW (b) PDF: TOGW

Fig. 15 Study B, PDF responses: OEW and TOGW

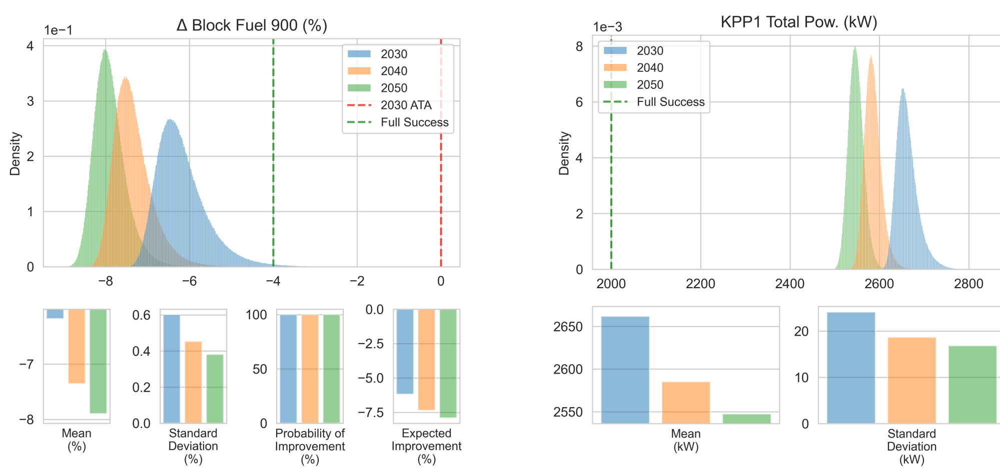

(a) PDF: Δ Block Fuel 900 (b) PDF: KPP1 Total Power

Fig. 16 Study B, PDF responses: Δ Block Fuel 900 nm mission and KPP1 Total Power

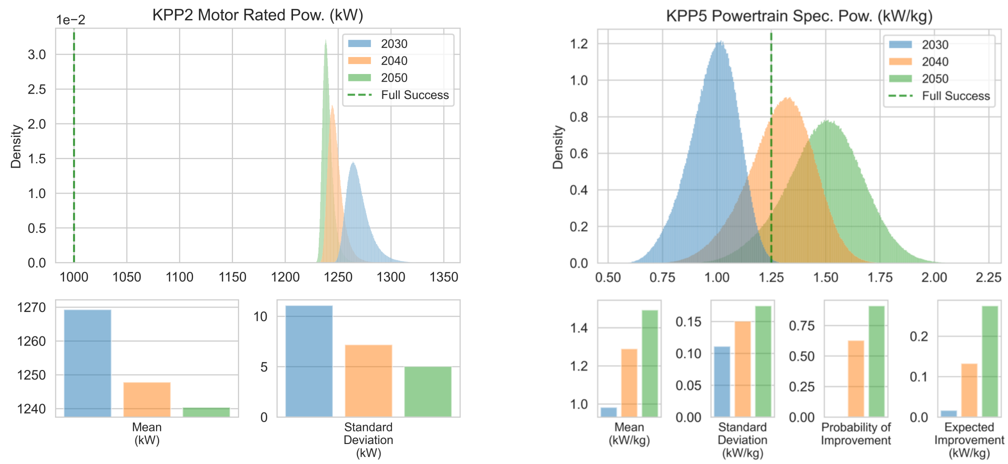

(a) PDF: KPP2 Motor Rated Pow.

(b) PDF: KPP5 Specific Power

Fig. 17 Study B, PDF responses: KPP2 Motor Rated Power and KPP5 Specific Power

Examining Fig. 18, it can be observed that battery k6, battery k8, and battery specific energy have a high contribution to variability of all responses, regardless of projection year. Thus, technological advancement in these battery parameters is vital to successful development of viable hybrid-electric transport aircraft. This intuitively makes sense as well since the ratio between battery k8 (technology parameter scaling battery max continuous current) and battery k6 (technology parameter scaling battery cell capacity) specifies the charge rate of the battery and the battery specific energy directly affects battery weight for a given power requirement. These parameters directly impact battery sizing, vehicle weight, and performance.

Also, it is evident that efficiency and specific power projections have a low contribution to overall variability, except for KPP1 (Total Power). Specifically, electrical machine efficiency emerges as a major contributor to overall variability of KPP1 as time moves forward. Thus, research and development aimed to increase KPP1 for hybrid-electric powertrains should be focused on improving the efficiency of electrical machines (motors or generators). The results in Fig. 18 are helpful because they inform future work by assisting in identification of critical inputs.

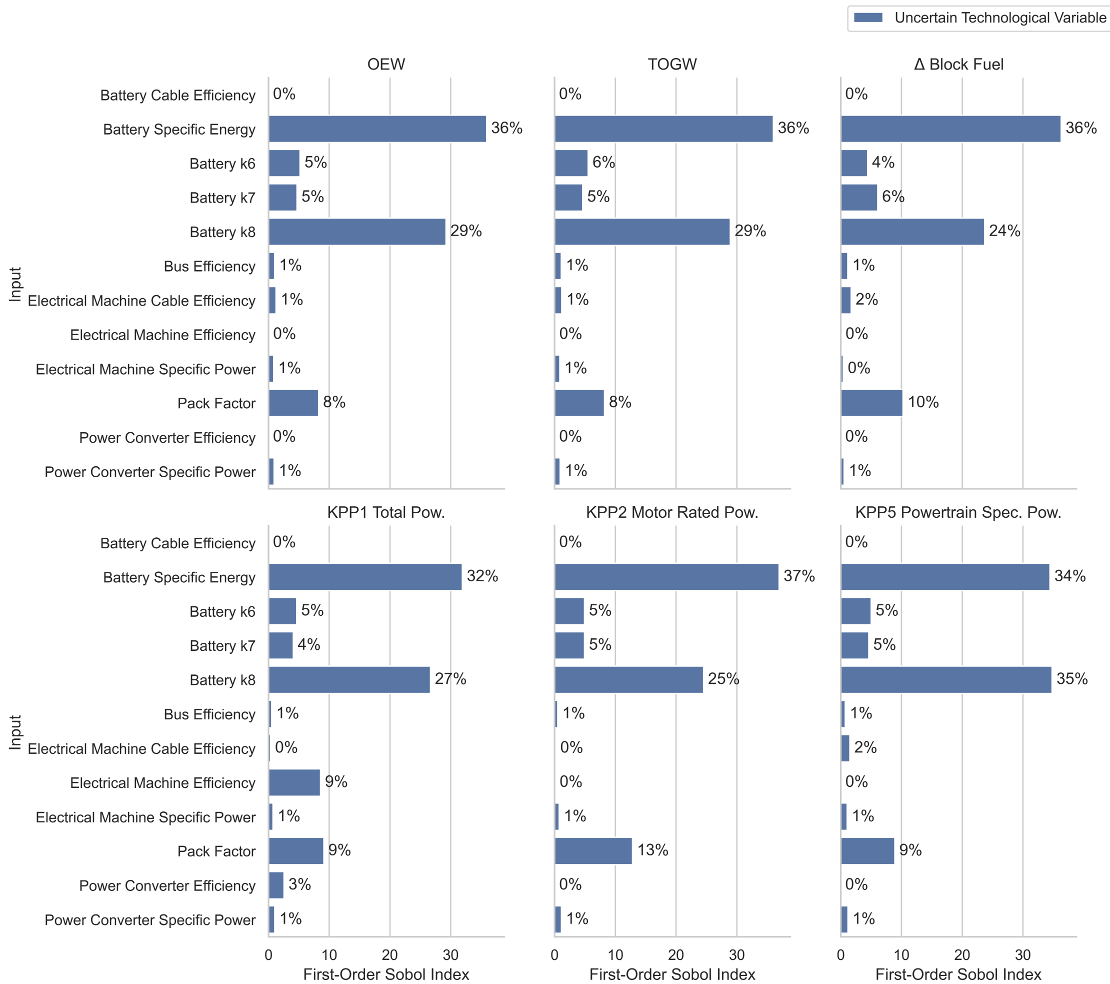

(a) Sobol Indices for Study B: 2030

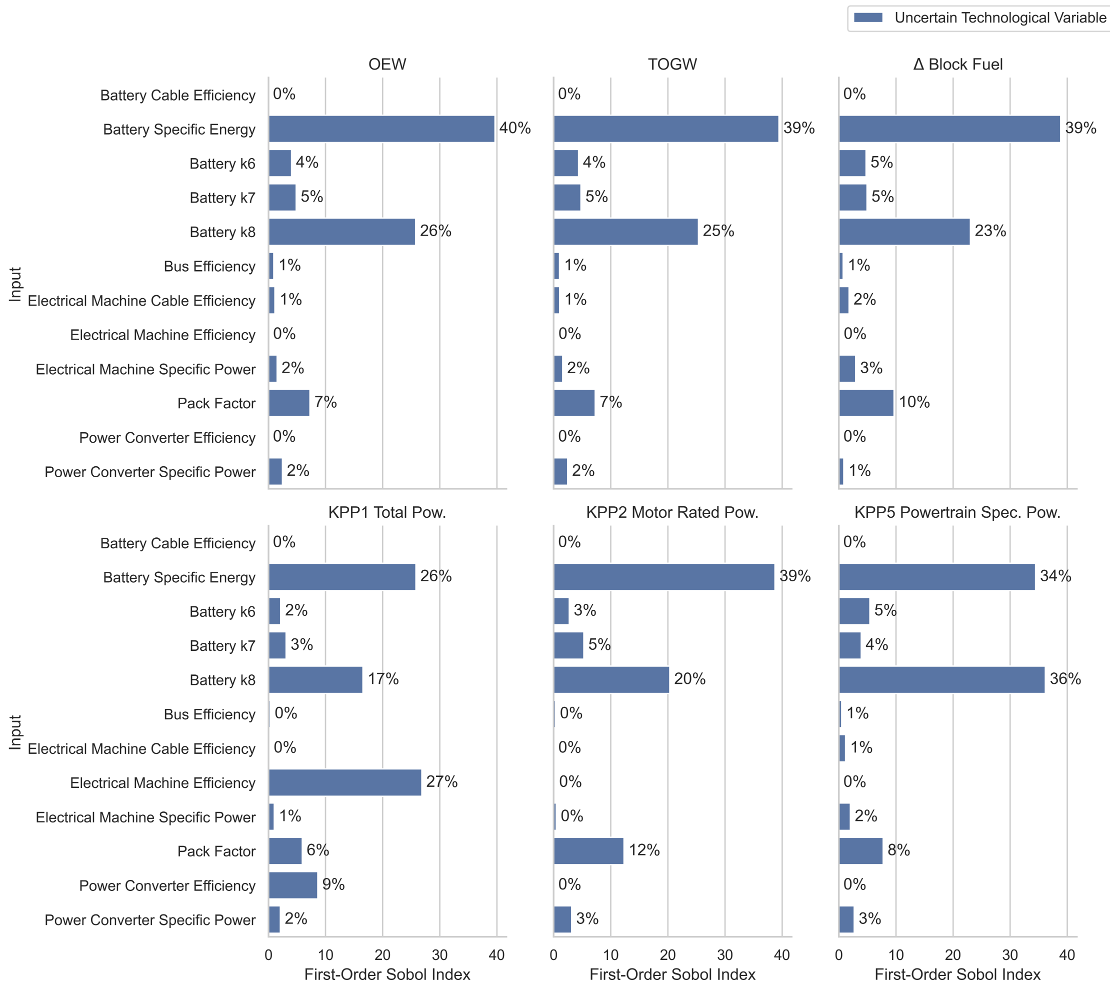

(b) Sobol Indices for Study B: 2040

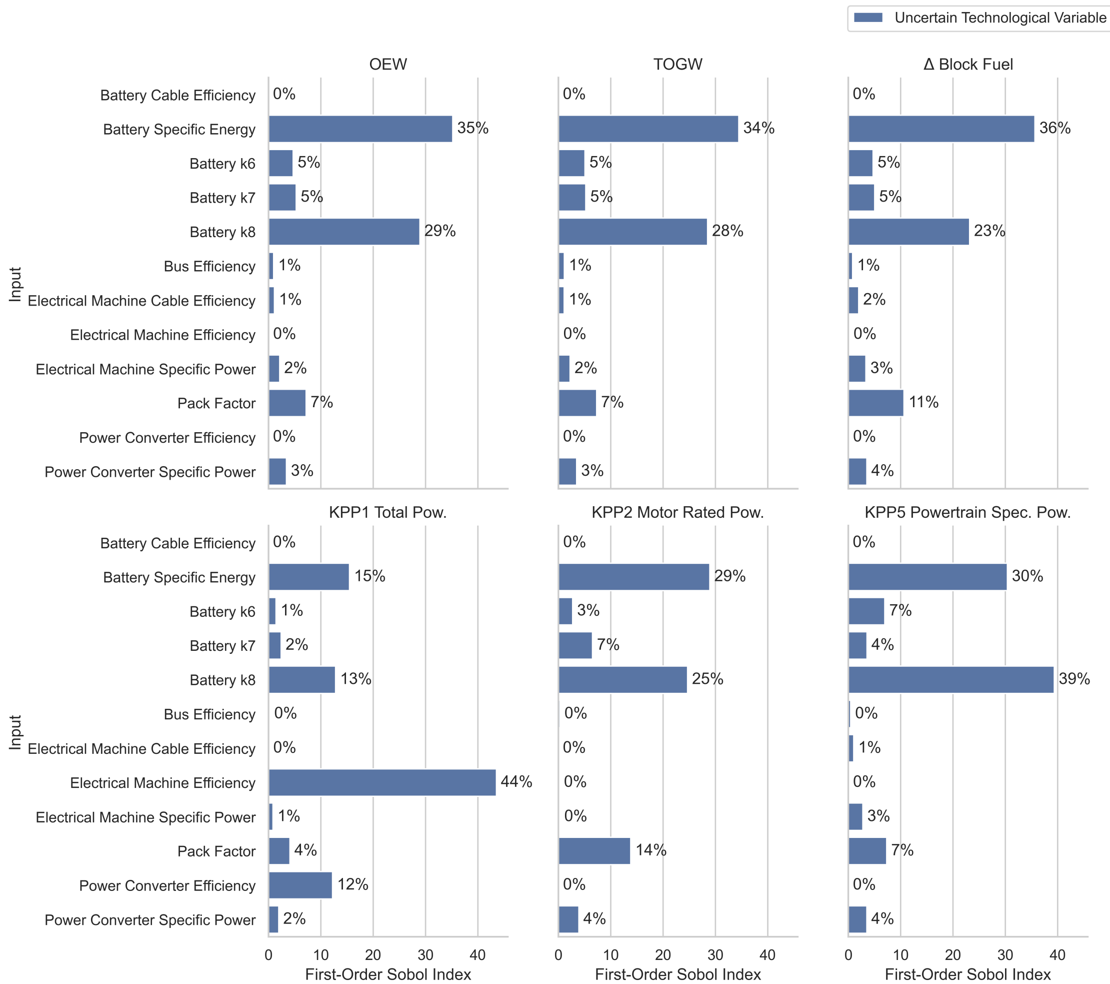

(c) Sobol Indices for Study B: 2050

Fig. 18 Sensitivity on EPFD responses with with different electrical parameter projections

V. Conclusion

There will always be uncertainty and risk associated with future technology development programs. Understanding the magnitude of that uncertainty allows to properly manage this risk. The methodology proposed in this work provides decision-makers with an initial framework to quantify risk brought on by technical sources of uncertainty. The authors will extend this framework to increase accuracy and improve upon the methodological formulation in this rapidly evolving area of study. The UQ analysis carried out on the EAP vehicle in this work provides an assessment of the most relevant technology uncertainty parameters to vehicle performance and quantifies uncertainty caused by those various factors. Results of the sensitivity study on the vehicle performance metrics due to technical uncertainties showed that responses were primarily driven by five technical uncertain inputs; however, most of the variability was shown to be driven by the battery specific energy parameter across the examined responses. This work provides a framework for assessing uncertainty on a 150-passenger vehicle in the EPFD problem context. The results indicate that improvements over the baseline vehicle are possible and become more significant in future time frames as battery specific energy and other uncertain electrical component parameters mature over time.

Acknowledgments

The authors would like to thank NASA for their support of this effort under AWD-002344 (NIA-602015), especially Gaudy Bezos-O'Connor, Ralph Jansen, and Fayette Collier. Additionally, the authors would like to thank graduate students Xiao (Olin) Wei, Daniel Nwachukwu, Lloyd Teta, and Fahraan Badruddin (School of Aerospace Engineering at Georgia Tech) for their contributions to this study.

References

[1] McDonald, R. A., German, B. J., Takahashi, T., Bil, C., Anemaat, W., Chaput, A., Vos, R., and Harrison, N., "Future aircraft concepts and design methods," *The Aeronautical Journal*, Vol. 126, No. 1295, 2022, p. 92–124. https://doi.org/10.1017/aer.2021.110.

[2] Overton, J., "Fact Sheet | The Growth in Greenhouse Gas Emissions from Commercial Aviation," 2019.

[3] "Paris Agreement," United Nations Climate Change, 2019.

[4] Botti, J., "Hybrid Electric Aircraft to Improve Environmental Impacts of General Aviation," June 2020.

[5] Tiede, B., O'Meara, C., and Jansen, R., "Battery Key Performance Projections based on Historical Trends and Chemistries," *2022 IEEE Transportation Electrification Conference Expo (ITEC)*, 2022, pp. 754–759. https://doi.org/10.1109/ITEC53557.2022.9814008.

[6] Hall, C., Pastra, C., Burrell, A., Gladin, J., and Mavris, D., "Projecting Power Converter Specific Power Through 2050 for Aerospace Applications," 2022, pp. 760–765. https://doi.org/10.1109/ITEC53557.2022.9813991.

[7] Pastra, C., Hall, C., Cinar, G., Gladin, J., and Mavris, D., "Specific Power and Efficiency Projections of Electric Machines and Circuit Protection Exploration for Aircraft Applications," 2022, pp. 766–771. https://doi.org/10.1109/ITEC53557.2022.9813927.

[8] Milios, K., Hall, C., Burrell, A., Brooks, J., Jr., J. K., Gladin, J., and Mavris, D., "Modeling and Simulation of a Parallel Hybrid-Electric Propulsion System - Electrified Powertrain Flight Demonstration (EPFD) Program," *IEEE/ AIAA Transportation Electrification Conf. and Electric Aircraft Tech. Symp*, Anaheim, CA, 2022.

[9] Nunez, L. S., Tai, J. C., and Mavris, D. N., *The Environmental Design Space: Modeling and Performance Updates*, AIAA, 2021. https://doi.org/10.2514/6.2021-1422.

[10] Sobol, I. M., "Sensitivity analysis for nonlinear mathematical models," *Math. Model. Comput. Exp*, Vol. 1, 1993, pp. 407–414.

[11] Saltelli, A., "Making best use of model evaluations to compute sensitivity indices," *Computer Physics Communication*, Vol. 145, 2002, pp. 280–297.

[12] Johnson, D., "The triangular distribution as a proxy for the beta distribution in risk analysis," *Journal of the Royal Statistical Society: Series D (The Statistician)*, Vol. 46, 2002, pp. 387 – 398. https://doi.org/10.1111/1467-9884.00091.

[13] Williams, T., "Practical Use of Distributions in Network Analysis," *Journal of the Operational Research Society*, Vol. 43, 1992, pp. 265–270.